Determining the Short Laser Pulse Contrast Based on X-Ray Emission Spectroscopy

A.S. Martynenko[1], I.Yu. Skobelev[1,2], S.A. Pikuz[1,2,*], S.N. Ryazantsev[1,2], C. Baird[3], N. Booth[4], L. Doehl[3], P. Durey[3], D. Farley[3], R. Kodama[5], K. Lancaster[3], P. McKenna[6], C. Murphy[3], C. Spindloe[4], T.A. Pikuz[1,5], and N. Woolsey[3]

[1] Joint Institute for High Temperatures of Russian Academy of Sciences, 125412 Moscow, Russia;
[2] National Research Nuclear University MEPhI, Kashirskoe Sh. 31, 115409 Moscow, Russia;
[3] York Plasma Institute, Department of Physics, University of York, York YO10 5DD, UK;
[4] Central Laser Facility, STFC Rutherford Appleton Laboratory, Didcot OX11 0QX, UK;
[5] Open and Transdisciplinary Research Initiative, Osaka University, Osaka 565-0871, Japan;
[6] Department of Physics, SUPA, University of Strathclyde, Glasgow G4 0NG, UK;
* Correspondence: spikuz@gmail.com

Abstract: The interaction of high-power short lasers with solid density targets is an important application of modern solid state lasers. However, uncertainties in measurements due to lack of information on the laser pedestal-to-peak contrast limits the validity of many conclusions. We show that X-ray spectral measurements can provide a straightforward way for accessing the laser pedestal-to-peak contrast. The experiments use silicon targets and relativistic laser intensities of 3×10^{20} W/cm^2 with a pulse duration of 1 ps. By not using or using a plasma mirror we compare low and high contrast measurements of the Ly-α line and its satellites to show that these lines are an effective laser contrast diagnostic. This diagnostic has potential to reduce uncertainty in future laser-solid interaction studies.

Keywords: laser contrast control; X-ray emission spectroscopy; plasma diagnostics; strong field laser physics; relativistic laser plasma.

1. Introduction

Studies of high energy density matter, where the energy density exceeds 1 Mbar or 10^5 J/cm^3, is necessary in many fields of science such as astrophysics, plasma physics, thermonuclear fusion, and accelerator physics (see, for example, Ref. [1,2]). Compression of preheated matter often in the form of a plasma by shock waves drive by, for example, gas guns, electrical pinch discharges, and high-power lasers is an often-used method for producing such conditions in the laboratory. With the development of short and ultra-short pulse lasers, it is possible to heat solid density materials to high temperatures before it significantly expands. In these situations, it is possible to reach high energy densities, at least for a short period of time, without needing to compress a target.

If the drive laser pulse duration τ_{las} is relatively short, then the plasma expands only to a distance of the order of an initial plasma size during τ_{las}, then the highest values of energy density possible will be achieved. For example, if a heating laser with a wavelength of 1 μm is used, then the initial plasma thickness (the thickness of a skin layer) will be of the order of $l_0 \sim 0.1$ μm, the τ_{las} must satisfy the criterion $\tau_{las} < l_0/v_f \sim$ (1-10) ps (for the average expansion velocity, taken as the speed of sound, $v_f \sim 10^6$-10^7 cm/s).

Plasma energy density depends on its temperature which, in turn, depends on the laser power. Increasing the total power of existing laser facilities is expensive. It is more economical to increase the laser power by decreasing the pulse duration (from the nanosecond to the picosecond and femtosecond range). This approach, using chirped pulse amplification (CPA), is the most widely used one for creating ultrahigh energy density states.

Despite the short duration, the criterion $\tau_{las} < l_0/v_f$ is not satisfied automatically for, say, picosecond laser pulses since the intensity-temporal profile of a picosecond laser pulse cannot be precisely controlled. We illustrate, schematically, in **Fig. 1**, that a high power laser pulse consists of pre-pulses of the order of a nanosecond before the main peak of the laser pulse (here we use the term "a nanosecond pre-pulse") and there is typically also a pedestal, labeled ASE for amplified spontaneous emission, directly adjacent to the laser peak with a duration of the order of 10 to 100 ps.

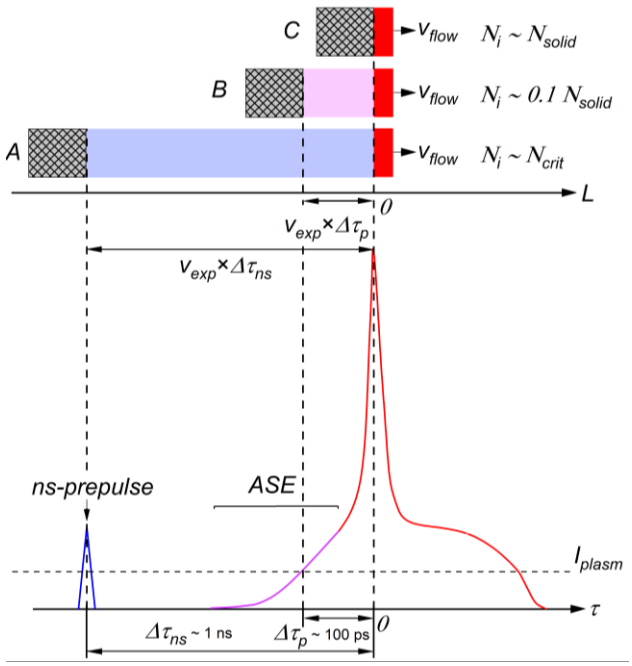

Fig. 1. Schematic of a laser pulse profile (bottom) and the resulting preplasma that forms by the time of arrival of the main pulse. Three different moments of preplasma expansion are illustrated. The peak of the main laser pulse arrives at "0": **A**, a preplasma (blue region) is generated by a nanosecond prepulse and expands for $\Delta\tau_{ns} \sim 1$ ns; **B**, a preplasma (pink region) is generated by a laser pedestal of amplified

spontaneous emission and expanded for $\Delta\tau_p \sim 0.1$ ns; and **C**, a preplasma is not formed at the moment of the peak laser pulse arrival; this occurs if the nanosecond pre-pulse and the pedestal are suppressed below the plasma formation threshold. The horizontal dashed line indicates the plasma formation boundary (marked as I_{plasm}) for cases **A** and **B**.

The intensity of the nanosecond pre-pulse is often sufficient to exceed the threshold intensity for plasma formation, which is approximately 10^{11} W/cm^2 for Si, and generates a preplasma early in the laser-target interaction. The preplasma expands greatly before the moment of the main laser pulse arrival, such that the energy of the pulse is absorbed in a long length scale plasma at and before the region of the critical density (with ion density $\sim 10^{20}$ cm^{-3} for $Z_n \sim 10$). Plasma energy density is relatively low in this scenario. Fortunately, the use of optical parametric CPA or OPCPA laser technology [3,4] can ensure the absence of the nanosecond prepulse.

Nevertheless, even for cases in which there is negligible nanosecond pre-pulse, the pedestal intensity can still exceed the plasma formation threshold causing a preplasma volume to increase in 10 to 100 ps ahead of the moment of the laser peak arrival, which will create an extended preplasma and a reduction in the plasma energy density.

It is a difficult, yet important, issue to understand the presence of a pedestal in any experiment and if at all possible to decrease the intensity of the pedestal. There are a few methods to reduce the picosecond pedestal: using a plasma mirror [5–10] or double plasma mirror [11]; using harmonics of the fundamental laser frequency [12]; nonlinear rotation of the plane of polarization [13,14]). As discussed above, the laser pedestal increases the preplasma and plasma density length scales; usually it is not possible to obtain data on the temporal-intensity laser pulse profile on a shot-to-shot basis, which is required to quantify this density decrease.

In the present work, we demonstrate that information on the laser pulse temporal-intensity profile can be inferred by characterizing the hot plasma density using X-ray emission spectral methods. This makes it possible to estimate the duration of the picosecond pedestal from the moment when the intensity exceeds the plasma formation threshold. The influence of the pedestal on the plasma density was experimentally investigated for laser intensities of approximately 3×10^{20} W/cm^2 and full-width-half maximum (FWHM) pulse duration of 1 ps. The intensity of the pedestal was varied by changing the laser contrast with a plasma mirror.

2. Experiment

We use the Vulcan petawatt Nd:glass facility [15] at the Rutherford Appleton Laboratory, UK. Laser pulses had energy on the target of about 300 J and FWHM duration (measured using a 3rd order autocorrelator) of about 1 ps. An off-axis parabola was used to achieve a spot diameter of about 7 μm which contains 30% of the laser energy on the target surface. The average laser intensity within the focal spot is 3×10^{20} W/cm^2. The angle of the laser incidence on the target

surface was 45°. The beam-target geometry and the alignment of the spectrometers is shown in **Fig. 2**. A more detailed scheme of the experiment is discussed in Ref. [16,17]. Solid Si foils of 0.5 μm thickness were used as targets. Using the OPCPA technology and a flat plasma mirror to improve the picosecond contrast of the laser achieves an ultrahigh laser contrast exceeding the value ~ 10^{10} at 1 ns [18]. As 50% of the laser energy can be lost in creating the plasma mirrors, plasma mirrors are not used regularly on OPCPA improved high-energy laser systems.

To measure the X-ray emission spectra from the front surface of the foils, we used three focusing spectrometers with spatial resolution (FSSR) [16,19,20] based on spherically curved α-quartz crystals and a photoluminescent plate or image plate as a detector. FSSRs were placed at an angle of 5^0 to the target normal. The observed spectral ranges of the three FSSRs were overlapping, which enabled measurement over a wide spectral range of 4.75–7.5 Å.

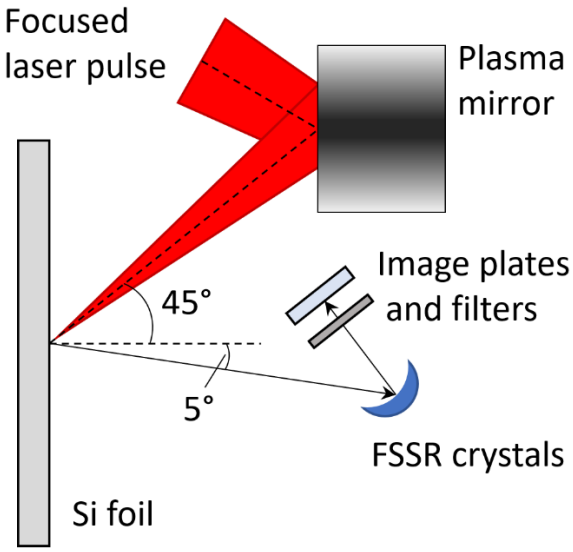

Fig. 2. Schematic of the experimental setup (not to scale). Relative positions of the target, the plasma mirror, and diagnostic FSSR spectrometers are shown.

3. Results

Two space and time integrated spectra are presented in **Fig. 3**. The first spectrum, shown as an orange line, corresponds to the case when using both OPCPA and the plasma mirror for a high contrast laser-target interaction, and the second spectrum was taken at low contrast by removing the plasma mirror. One can see that these spectra are markedly different. At high contrast the spectral line widths are broad and the Ly-like resonance lines appear brighter than the He-like resonance lines.

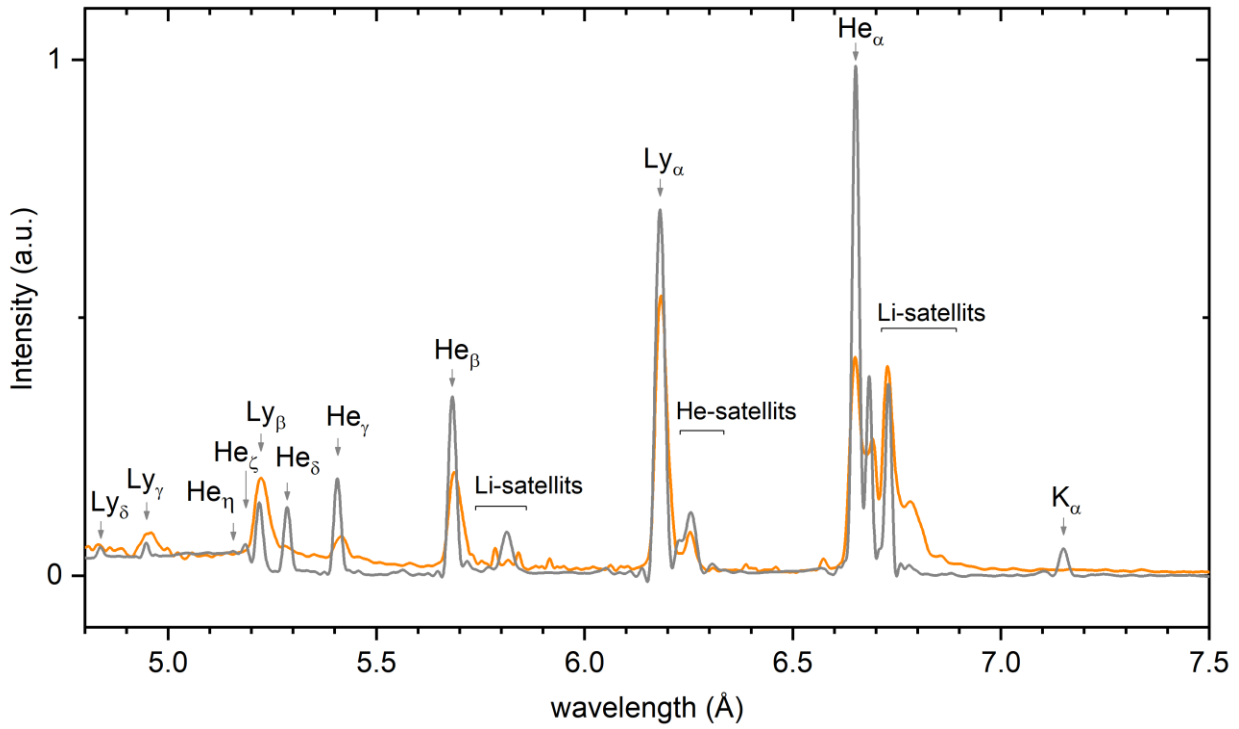

Fig. 3. Spectra of the picosecond laser plasma formed by laser pulses of different contrasts: a spectrum from a relatively high contrast is shown by the orange curve and compared to a spectrum from a relatively low contrast interaction by the black curve.

A convenient way of determining plasma density is using the dielectric satellite structure $2l2p$ - $1s2l$ of the H-like Si XIV ion resonance line. Relative lines intensities of these satellites are sensitive to plasma density and relatively insensitive to the plasma temperature, as was first shown in Ref [21]. Moreover, the plasma is usually optically thin to these satellites, and the satellite structure itself does not depend on the ionization state of the plasma. **Fig. 4** shows collisional-radiative calculations using the PrismSPECT code [22,23] of how the $2l2p$ - $1s2l$ satellite structure depends on plasma density and temperature.

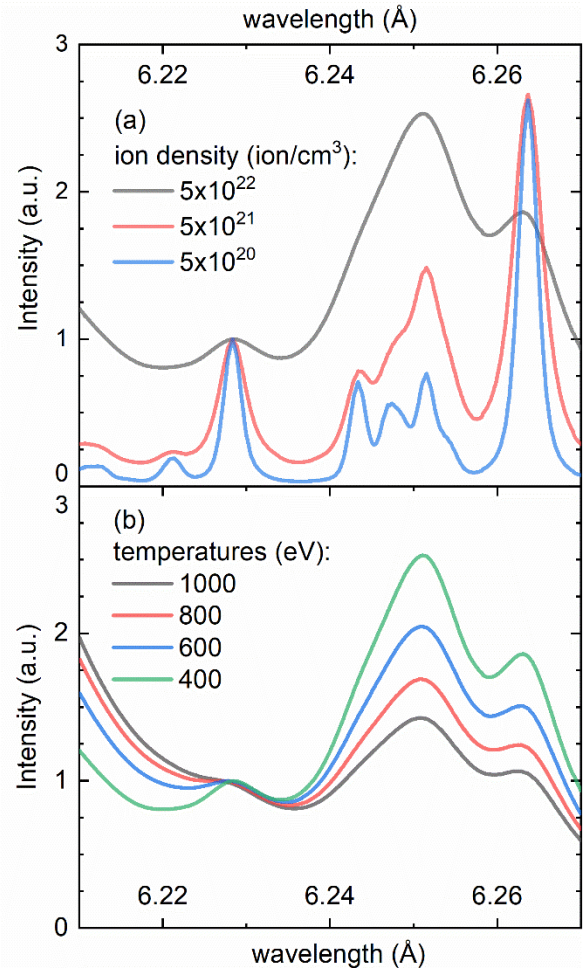

Fig. 4. (a) PrismSPECT calculations of the 2l2p - 1s2l satellite emission spectra from a Si plasma with a fixed temperature of 400 eV and ion densities in a range of 1×10^{20} cm^{-3} to 5.2×10^{22} cm^{-3}. **(b)** A set of calculated emission spectra of the Si plasma with fixed ion density of 3×10^{22} cm^{-3} and temperatures in a range of 300 to 1000 eV.

The ratio of the spectral line integrated intensities of the satellite structure to the resonance line is a robust plasma electron temperature T_e diagnostic. Analysis of an experimental spectrum allows one to simultaneously determine space and time averaged values of ion and electron density N_i, N_e using the $2l2p$ - $1s2l$ satellite structure and electron temperature T_e using the ratio of the resonance and satellite integrated intensities. A comparison between experimental and PrismSPECT Ly-α and satellite spectra in **Fig. 5** shows that it is possible to describe the satellite structure reasonably well, but not the widths of the observed spectral lines.

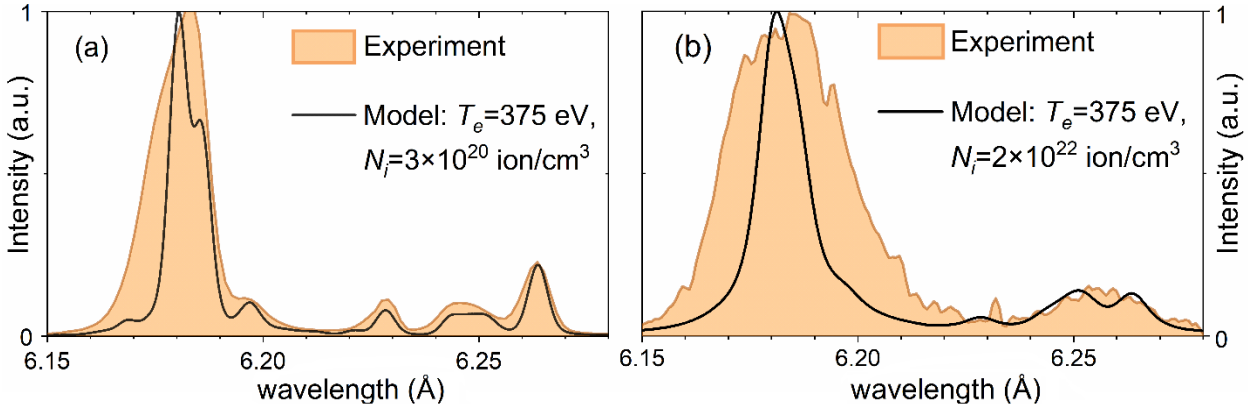

Fig. 5. Experimental data shown as the orange shaded region for **(a)** low and **(b)** high laser contrast laser-target interactions compared with calculated spectra as black curves, without inclusion of line broadening effect due to the plasma expansion. The satellite lines are best fit with electron temperature of 375 eV and ion number density of 3×10^{20} cm^{-3} and 2×10^{22} cm^{-3} respectively.

These calculations include spectral line broadening due to Stark and thermal Doppler effects, but not Doppler broadening due to macroscopic motion from the expansion of the plasma. Assuming a plasma average expansion velocity v_{exp} and that the velocity spread was of the order of v_{exp}, one can see in **Fig. 6(a)** that by including this as a broadening mechanism, the calculation results in a much better description of the experimental spectrum.

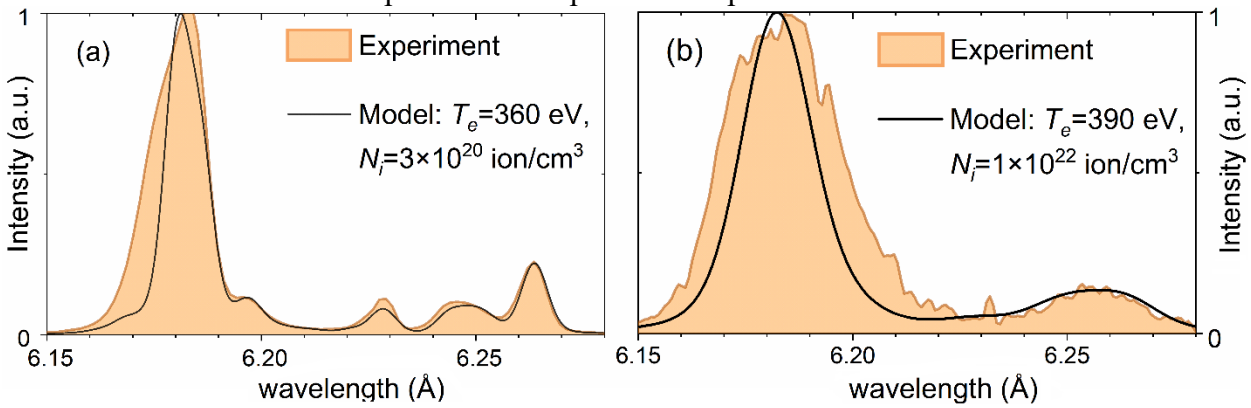

Fig. 6. Experimental data shown as the orange shaded region for **(a)** low and **(b)** high laser-target contrast compared with calculated spectra shown as black curves, with inclusion of line broadening effect due to the plasma expansion of 3×10^7 cm/s in order to obtain improved agreement between spectra.

In the case of a low laser contrast experiment (without using the plasma mirror), the best agreement between the experimental and calculated spectra was reached for $N_i = 3\times10^{20}$ cm^{-3}, $T_e = 360$ eV, and the expansion velocity of $v_{exp} = 3\times10^7$ cm/s, see **Fig. 6(a)**. Since the inferred ion density is more than 200 times lower than the solid-state one, the preplasma expands to greater distances than the focus spot diameter, hence, the expansion cannot be treated as a 1-dimensional planar expansion. We assume the plasma expands into a cone with opening of about ~ 90°, the

prepulse pedestal temporal duration was estimated as 25 ps from the moment of preplasma formation, which is in agreement with the data from Ref. [18]. The preplasma formation threshold was estimated from [24] to be in order of 10^{12} W/cm^2. Accordingly, the laser contrast for this shot was about 10^8 at 25 ps. It should be noted that electron density of the preplasma, in this case, is $N_e = (3\text{-}4) \times 10^{21}$ cm^{-3}, which is several times greater than the critical density. The main laser pulse propagates to relativistic corrected critical density of 1.6×10^{21} cm^{-3} (see, for example, Ref. [25–27]), to heat a significant mass of the preplasma.

In the case of a high laser contrast experiment, see **Fig. 6(b)** (with the plasma mirror), the best agreement between the experimental and calculated spectra was found for $N_i = 1\times10^{22}$ cm^{-3}, $T_e = 390$ eV, and an expansion velocity of $v_{exp} = 4.5 \times 10^7$ cm/s. The inferred ion density is approximately 5 times lower than the solid-state density; the expansion is treated as planar and one-dimensional, and the duration of the prepulse pedestal for laser intensities above the material threshold does not exceed 1 ps (in other words, laser contrast for this shot was about 10^8 at 1 ps). This is close to the FWHM duration of the main laser pulse. By using a plasma mirror, the switch-on time of the laser forming a plasma is delayed. This reduces the expansion of the preplasma, and also reduces the density lengths scales in region of the relativistic critical density where strong laser absorption occurs. If the plasma expansion is sufficiently small compared to the skin depth, then the main pulse can heat the solid density part of the target, which will lead to an increase in the average plasma density.

Although our density estimate was obtained using a simple approximation of the plasma expansion, it is consistent with the simulation results obtained using more sophisticated models of the expansion and cooling of the plasma [28]. It should be also noted that even when using a plasma mirror, the laser will interact with preplasma created by the remaining laser pedestal. As a result, the laser interacts with a plasma that is likely very dense yet below solid density. Intense laser interactions with solid-state density plasma is possible when using laser pulses with especially short duration femtosecond lasers [29], or by using special coated (buried in plastic) targets [30].

4. Discussion & conclusions

The results indicate clearly that commonly used schemes for generating picosecond duration laser pulses of relativistic intensity have nanosecond to picosecond pedestals with intensity and duration sufficient for the formation of a preplasma. The preplasma density varies with position approximately exponentially with critical density plasma scale length dependent on the contrast between the lasers pedestal and main peak intensity.

When using a plasma mirror, the pedestal intensity decreases, which leads to a significant reduction in the duration of the remaining part of the pedestal that interacts with the target at an intensity that exceeds the plasma formation threshold. Consequently, the scale length of the preplasma formed by such a “shortened” prepulse is smaller, and the average plasma density with

which the laser interacts increases. Observation of the plasma emission spectrum, especially in the region of the resonance line of Ly-like multiply charged ions, allows one to readily estimate the duration of the picosecond pedestal. This is potentially important in common situations where laser pulse contrast measurements are not otherwise available.

In conclusion, X-ray emission spectral measurements of a laser plasma allows one to diagnose plasma parameters as well as to estimate the short laser pulses characteristics itself. This technique is particularly relevant for creating states of matter with ultrahigh energy density.

The work of was done in the frame of State Assignment of Ministry for Science and Higher Education of Russia to JIHT RAS #075-00892-20-00. The work of UK team received financial support from UK EPSRC grants EP/L01663X/1 and EP/H012605/1.

References

[1] G.A. Mourou, T. Tajima, S. V. Bulanov, Optics in the relativistic regime, Rev. Mod. Phys. 78 (2006) 309–371. https://doi.org/10.1103/RevModPhys.78.309.

[2] V.E. Fortov, Extreme States of Matter, Springer International Publishing, Cham, 2016. https://doi.org/10.1007/978-3-319-18953-6.

[3] H.C. Kapteyn, M.M. Murnane, A. Szoke, R.W. Falcone, Prepulse energy suppression for high-energy ultrashort pulses using self-induced plasma shuttering, Opt. Lett. 16 (1991) 490–492. https://doi.org/0146-9592/91/070490-03$5.00/0.

[4] H. Kiriyama, M. Mori, Y. Nakai, T. Shimomura, M. Tanoue, A. Akutsu, S. Kondo, S. Kanazawa, H. Okada, T. Motomura, H. Daido, T. Kimura, T. Tajima, High-contrast, high-intensity laser pulse generation using a nonlinear preamplifier in a Ti:sapphire laser system, Opt. Lett. 33 (2008) 645. https://doi.org/10.1364/OL.33.000645.

[5] D. Riley, J.J. Angulo-Gareta, F.Y. Khattak, M.J. Lamb, P.S. Foster, E.J. Divall, C.J. Hooker, A.J. Langley, R.J. Clarke, D. Neely, Kα yields from Ti foils irradiated with ultrashort laser pulses, Phys. Rev. E. 71 (2005) 016406. https://doi.org/10.1103/PhysRevE.71.016406.

[6] K.B. Wharton, C.D. Boley, A.M. Komashko, A.M. Rubenchik, J. Zweiback, J. Crane, G. Hays, T.E. Cowan, T. Ditmire, Effects of nonionizing prepulses in high-intensity laser-solid interactions, Phys. Rev. E. 64 (2001) 025401. https://doi.org/10.1103/PhysRevE.64.025401.

[7] A.L. Kritcher, P. Neumayer, M.K. Urry, H. Robey, C. Niemann, O.L. Landen, E. Morse, S.H. Glenzer, K-alpha conversion efficiency measurements for X-ray scattering in inertial confinement fusion plasmas, High Energy Density Phys. 3 (2007) 156–162. https://doi.org/10.1016/j.hedp.2007.02.012.

[8] S.N. Chen, G. Gregori, P.K. Patel, H.-K. Chung, R.G. Evans, R.R. Freeman, E. Garcia Saiz, S.H. Glenzer, S.B. Hansen, F.Y. Khattak, J.A. King, A.J. Mackinnon, M.M. Notley, J.R. Pasley, D. Riley, R.B. Stephens, R.L. Weber, S.C. Wilks, F.N. Beg, Creation of hot dense matter in short-pulse laser-plasma interaction with tamped titanium foils, Phys. Plasmas. 14 (2007) 102701. https://doi.org/10.1063/1.2777118.

[9] G. Doumy, F. Quéré, O. Gobert, M. Perdrix, P. Martin, P. Audebert, J.C. Gauthier, J.-P. Geindre, T. Wittmann, Complete characterization of a plasma mirror for the production of high-contrast ultraintense laser pulses, Phys. Rev. E. 69 (2004) 026402. https://doi.org/10.1103/PhysRevE.69.026402.

[10] R. Hörlein, B. Dromey, D. Adams, Y. Nomura, S. Kar, K. Markey, P. Foster, D. Neely, F. Krausz, G.D. Tsakiris, M. Zepf, High contrast plasma mirror: spatial filtering and second harmonic generation at 10 19 W cm −2, New J. Phys. 10 (2008) 083002. https://doi.org/10.1088/1367-2630/10/8/083002.

[11] I. Kim, I.W. Choi, S.K. Lee, K.A. Janulewicz, J.H. Sung, T.J. Yu, H.T. Kim, H. Yun, T.M. Jeong, J. Lee, Spatio-temporal characterization of double plasma mirror for ultrahigh contrast and stable laser pulse, Appl. Phys. B. 104 (2011) 81–86. https://doi.org/10.1007/s00340-011-4584-2.

[12] A. Jullien, O. Albert, F. Burgy, G. Hamoniaux, J.-P. Rousseau, J.-P. Chambaret, F. Augé-Rochereau, G. Chériaux, J. Etchepare, N. Minkovski, S.M. Saltiel, 10^?10 temporal contrast for femtosecond ultraintense lasers by cross-polarized wave generation, Opt. Lett. 30 (2005) 920. https://doi.org/10.1364/OL.30.000920.

[13] J.-L. Tapié, G. Mourou, Shaping of clean, femtosecond pulses at 1053 µm for chirped-pulse amplification, Opt. Lett. 17 (1992) 136. https://doi.org/10.1364/OL.17.000136.
[14] D. Homoelle, M. Foster, A.L. Gaeta, V. Yanovsky, G. Mourou, Pulse contrast enhancement of high-energy pulses using a gas-filled hollow waveguide, in: Summ. Pap. Present. Lasers Electro-Optics. CLEO '02. Tech. Diges, Opt. Soc. America, 2002: pp. CPDA4-1-CPDA4-3. https://doi.org/10.1109/CLEO.2002.1034468.
[15] C.N. Danson, P.A. Brummitt, R.J. Clarke, J.L. Collier, B. Fell, A.J. Frackiewicz, S. Hancock, S. Hawkes, C. Hernandez-Gomez, P. Holligan, M.H.R. Hutchinson, A. Kidd, W.J. Lester, I.O. Musgrave, D. Neely, D.R. Neville, P.A. Norreys, D.A. Pepler, C.J. Reason, W. Shaikh, T.B. Winstone, R.W.W. Wyatt, B.E. Wyborn, Vulcan petawatt - An ultra-high-intensity interaction facility, Nucl. Fusion. 44 (2004) S239–S246. https://doi.org/10.1088/0029-5515/44/12/S15.
[16] I.Y. Skobelev, S.N. Ryazantsev, D.D. Arich, P.S. Bratchenko, A.Y. Faenov, T.A. Pikuz, P. Durey, L. Doehl, D. Farley, C.D. Baird, K.L. Lancaster, C.D. Murphy, N. Booth, C. Spindloe, P. McKenna, S.B. Hansen, J. Colgan, R. Kodama, N. Woolsey, S.A. Pikuz, X-ray absorption spectroscopy study of energy transport in foil targets heated by petawatt laser pulses, Photonics Res. 6 (2018) 234. https://doi.org/10.1364/PRJ.6.000234.
[17] A.S. Martynenko, S.A. Pikuz, I.Y. Skobelev, S.N. Ryazantsev, C. Baird, N. Booth, L. Doehl, P. Durey, A.Y. Faenov, D. Farley, R. Kodama, K. Lancaster, P. McKenna, C.D. Murphy, C. Spindloe, T.A. Pikuz, N. Woolsey, Optimization of a laser plasma-based X-ray source according to WDM absorption spectroscopy requirements, Matter Radiat. Extrem. (2020).
[18] C. Hernandez-Gomez, Overview of the Central Laser Facility (CLF), in: CLF Annu. Rep. 2016-2017, 2017: pp. 6–8.
[19] A.Y. Faenov, S.A. Pikuz, A.I. Erko, B.A. Bryunetkin, V.M. Dyakin, G. V Ivanenkov, A.R. Mingaleev, T.A. Pikuz, V.M. Romanova, T.A. Shelkovenko, High-performance x-ray spectroscopic devices for plasma microsources investigations, Phys. Scr. 50 (1994) 333–338. https://doi.org/10.1088/0031-8949/50/4/003.
[20] M.A. Alkhimova, I.Y. Skobelev, A.Y. Faenov, D.A. Arich, T.A. Pikuz, S.A. Pikuz, Accounting for the instrument function of crystal spectrometers operating in many reflection orders in the diagnostics of laser plasma from its continuum spectrum, Quantum Electron. 48 (2018) 749–754. https://doi.org/10.1070/QEL16675.
[21] V.I. Bayanov, V.A. Boiko, A.V. Vinogradov, S.S. Gulidov, A.A. Ilyukhin, V.A. Katulin, A.A. Mak, V.Y. Nosach, A.L. Petrov, G.V. Peregudov, S.A. Pikuz, I.Y. Skobelev, A.D. Starikov, A.Y. Faenov, V.A. Chirkov, E.A. Yukov, Anomalous intensities of satellites of resonance lines of hydrogen-like ions, JETP Lett. 24 (1976) 319–324.
[22] J.J. MacFarlane, I.E. Golovkin, P.R. Woodruff, D.R. Welch, B. V Oliver, T.A. Mehlhorn, R.B. Campbell, Simulation of the ionization dynamics of aluminum irradiated by intense short-pulse lasers, in: Proc. Third Inert. Conf. Inert. Fusion Sci. Appl. 2003, 2003: pp. 1–4. http://www.prism-cs.com/.
[23] J.J. MacFarlane, I.E. Golovkin, P. Wang, P.R. Woodruff, N.A. Pereyra, SPECT3D - A multi-dimensional collisional-radiative code for generating diagnostic signatures based on hydrodynamics and PIC simulation output, High Energy Density Phys. 3 (2007) 181. https://doi.org/10.1016/j.hedp.2007.02.016.
[24] M.F. Ciappina, S. V. Popruzhenko, S. V. Bulanov, T. Ditmire, G. Korn, S. Weber, Progress

toward atomic diagnostics of ultrahigh laser intensities, Phys. Rev. A. (2019). https://doi.org/10.1103/PhysRevA.99.043405.

[25] A.Y. Faenov, J. Colgan, S.B. Hansen, A. Zhidkov, T.A. Pikuz, M. Nishiuchi, S.A. Pikuz, I.Y. Skobelev, J. Abdallah, H. Sakaki, A. Sagisaka, A.S. Pirozhkov, K. Ogura, Y. Fukuda, M. Kanasaki, N. Hasegawa, M. Nishikino, M. Kando, Y. Watanabe, T. Kawachi, S. Masuda, T. Hosokai, R. Kodama, K. Kondo, Nonlinear increase of X-ray intensities from thin foils irradiated with a 200 TW femtosecond laser, Sci. Rep. 5 (2015) 13436. https://doi.org/10.1038/srep13436.

[26] M.A. Alkhimova, A.Y. Faenov, I.Y. Skobelev, T.A. Pikuz, M. Nishiuchi, H. Sakaki, A.S. Pirozhkov, A. Sagisaka, N.P. Dover, K. Kondo, K. Ogura, Y. Fukuda, H. Kiriyama, K. Nishitani, T. Miyahara, Y. Watanabe, S.A. Pikuz, M. Kando, R. Kodama, K. Kondo, High resolution X-ray spectra of stainless steel foils irradiated by femtosecond laser pulses with ultra-relativistic intensities, Opt. Express. 25 (2017) 29501. https://doi.org/10.1364/OE.25.029501.

[27] E. Oks, E. Dalimier, A.Y. Faenov, P. Angelo, S.A. Pikuz, T.A. Pikuz, I.Y. Skobelev, S.N. Ryazanzev, P. Durey, L. Doehl, D. Farley, C. Baird, K.L. Lancaster, C.D. Murphy, N. Booth, C. Spindloe, P. McKenna, N. Neumann, M. Roth, R. Kodama, N. Woolsey, In-depth study of intra-Stark spectroscopy in the x-ray range in relativistic laser-plasma interactions, J. Phys. B At. Mol. Opt. Phys. 50 (2017) 245006. https://doi.org/10.1088/1361-6455/aa93c7.

[28] A.S. Martynenko, I.Y. Skobelev, S.A. Pikuz, Possibility of estimating high-intensity-laser plasma parameters by modelling spectral line profiles in spatially and time-integrated X-ray emission, Appl. Phys. B. 125 (2019) 31. https://doi.org/10.1007/s00340-019-7149-4.

[29] S.A. Pikuz, I.Y. Skobelev, M.A. Alkhimova, G. V. Pokrovskii, J. Colgan, T.A. Pikuz, A.Y. Faenov, A.A. Soloviev, K.F. Burdonov, A.A. Eremeev, A.D. Sladko, R.R. Osmanov, M. V. Starodubtsev, V.N. Ginzburg, A.A. Kuz'min, A.M. Sergeev, J. Fuchs, E.A. Khazanov, A.A. Shaikin, I.A. Shaikin, I. V. Yakovlev, Formation of a plasma with the determining role of radiative processes in thin foils irradiated by a pulse of the PEARL subpetawatt laser, JETP Lett. 105 (2017) 13–17. https://doi.org/10.1134/S0021364017010131.

[30] A.S. Martynenko, S.A. Pikuz, I.Y. Skobelev, S.N. Ryazantsev, C. Baird, N. Booth, L. Doehl, P. Durey, A.Y. Faenov, D. Farley, R. Kodama, K. Lancaster, P. McKenna, C.D. Murphy, C. Spindloe, T.A. Pikuz, N. Woolsey, Effect of plastic coating on the density of plasma formed in Si foil targets irradiated by ultra-high-contrast relativistic laser pulses, Phys. Rev. E. 101 (2020) 043208. https://doi.org/10.1103/PhysRevE.101.043208.